Strain methods for changing local electric field gradient in $BaFe_2As_2$

C. Williams, C. Chaffey, and N.J. Curro
Department of Physics and Astronomy, University of California, Davis

In this study, we introduce a novel approach aimed at advancing the investigation of local nematicity in $BaFe_2As_2$ via dynamically pulsed strain fields. Our research is motivated by the pursuit of a more sensitive alternative to existing static strain methods. Employing nuclear magnetic resonance techniques, we measure the nuclear quadrupolar energy splittings, utilizing them as a sensitive indicator of the electric field gradient (EFG) that couples strongly to the orbital occupations of the ^{75}As p-orbitals. In the new method, we discern an EFG response through changes in the phase acquired by the nuclear magnetization while time-evolving in the strain field, as opposed to a change in resonance frequency under constant strain. The previous technique measured a linear response in the EFG to applied strain and extracted the nematic susceptibility from these slopes as a function of temperature. The susceptibility diverged near the known structural transition and agreed with elastoresistance measurements. Our technique replicates the static results but proves three orders of magnitude more sensitive and hence requires less strain, establishing possible use for materials with a wider range of physical properties.

Introduction

In the absence of a strain field, $BaFe_2As_2$ undergoes a weak first order antiferromagnetic phase transition and a lattice distortion at around 135K [1]. The original tetragonal symmetry of the crystal is broken and results in an orthorhombic structure, lifting the degeneracy of certain Fe d-orbitals, a phenomenon closely related to the development of antiferromagnetism. The ordered regime is preceded by a divergence of nematic susceptibility as temperature is lowered through the disordered phase. Thus, this crystal like other iron-based superconductors, exhibits a dance of orbital, magnetic, and lattice degrees of freedom, making it difficult for low energy probes to provide quantitative analysis.

We are particularly interested in examining nematic degrees of freedom. The ^{75}As quadrupolar moment couples closely with the EFG, making it a sensitive probe of the Fe d-orbital occupations. Applying strain to $BaFe_2As_2$ creates an asymmetric EFG, and we define an asymmetry parameter η as:

$$\eta = \frac{V_{aa} - V_{bb}}{V_{aa} + V_{bb}} \tag{1}$$

where V_{aa} and V_{bb} refer to the EFG in the [100] (a) and [010] (b) crystal directions in the orthorombic phase [2]. Strain breaks the tetragonal symmetry of the EFG, similar to the zero strain EFG behavior at the phase transition, and therefore affects the quadrupolar interaction with the nucleus. Static strain is applied via a RazorbillTM CS100 piezoelectric strain device and we analyze the quadrupolar interaction by measuring the difference between the satellite transition frequency and the central transition frequency with our radiofrequency field and strain applied along one of the directions. We call this difference the quadrupolar splitting, depicted in Fig 1, and it is proportional to our asymmetry parameter η. Fig 1 shows the field swept spectra for the satellite transitions when we hold the crystal at various displacements.

We look to introduce a pulsed strain sequence, in the form of a square wave alternating between positive and negative strain of the same magnitude, through the same piezo device.

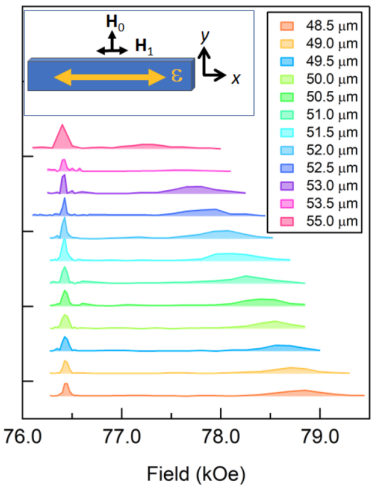

FIG. 1: Used with permission from [2]. Field-swept spectra of $BaFe_2As_2$ at constant frequency f = 55.924 MHz at 138 K for several different displacements, showing the center and upper satellite transitions. Inset: Orientation of the crystal with respect to the external field, H_0, the strain axis, and the rf field H_1. Zero strain corresponds to 51.58μm.[2].

Strain is a dimensionless quantity given as the ratio of a sample's displacement divided by its total length. Because η is linearly proportional to strain, ϵ, it will change the phase acquired by the nuclear magnetization while time-evolving in the strain field rather than producing a measurable shift in the resonance frequency. To observe a difference in the resonance frequency due to static strain, the field should force a frequency shift equal to or greater than the width of the original spectrum $\frac{1}{T_2^*}$:

$$\delta f = (\frac{df}{d\epsilon_s})\epsilon_s \gtrsim \frac{1}{T_2^*} \tag{2}$$

where we measured $\frac{1}{T_2^*}$ in $BaFe_2As_2$ to be approximately 300

kHz $\sim \frac{1}{3}\mu$s. Thus, the minimum required strain is:

$$\epsilon_{min} \gtrsim (\frac{df}{d\epsilon_s})^{-1}(T_2^*)^{-1} \sim (\frac{df}{d\epsilon_s})^{-1}(3.3 * 10^6) \quad (3)$$

As mentioned prior, our pulsed technique picks up changes in phase arising from change in frequency. The phase acquired due to a pulsed strain sequence is:

$$\delta\theta \gtrsim 2t_{pulse}(\frac{df}{d\epsilon_p})\epsilon_p \quad (4)$$

where t_{pulse} is the amount of time the strain pulse is applied. In our case this is optimized at $t_{pulse} \sim 900\mu s$ for reasons we will get to later. Our experiment has an uncertainty of approximately five degrees when measuring phase, therefore the minimum strain required to overcome this uncertainty is:

$$\epsilon_{min} \gtrsim \frac{5(df/d\epsilon_p)^{-1}}{2t_{pulse}} \sim (\frac{df}{d\epsilon_s})^{-1}(2.7 * 10^3) \quad (5)$$

The factor of $\frac{df}{d\epsilon}$ will not change between the two methods when looking at a particular peak. We see that phase detection could be as many as three orders of magnitude more sensitive, hence requiring less strain. Quantum simulations indicate that measuring this phase is possible, so we design an experiment to test the theory. Here we cover the technical methods of nuclear magnetic resonance (NMR), simulated results, and a survey of applied strain.

Nuclear Magnetic Resonance

Our experiment utilizes the Hahn echo pulse sequence, a fundamental technique commonly employed in NMR spectroscopy. This method is particularly useful for mitigating the influence of inhomogeneous broadening in a spectrum.

In the Hahn echo sequence, a radiofrequency (RF) pulse is applied to a sample, in our case $BaFe_2As_2$, where the nuclear spins are in an eigenstate of the system. More specifically, we use a powerful electromagnet to create a field we call H_0 that causes a net magnetization due to the Zeeman effect in a direction we denote as the z direction. We then apply an RF pulse to a coil wrapped around the sample. The energy from this RF pulse can be absorbed by a nucleus. When the pulse is applied for the correct amount of time, it orchestrates a rotation of the nuclear spins (and the net magnetization they constitute) away from the z-axis and into the xy plane. t_{90} refers to the duration of the RF pulse that will rotate the spins by 90 degrees. Once in plane, the spins precess at the Larmor frequency, the same frequency as the t_{90} RF pulse and hence referred to as the nuclear resonance frequency.

A wait time, τ, is introduced, and the nuclear spins begin losing their original phase coherence due to spin-spin and spin-lattice interactions. The loss of coherence and decrease in net magnetization is known as 'spin-dephasing'. To counteract this dephasing, a second RF pulse is applied after the τ interval. This pulse matches the frequency of the first but is applied for twice as long, a duration we call t_{180}, in order to rotate the nuclear spins an additional 180 degrees. Doing so inverts the phase and causes the spins that were previously furthest ahead to now be furthest behind (Fig 2). The inversion causes the previously dephasing spins to refocus and form an echo signal, which occurs at time 2τ.

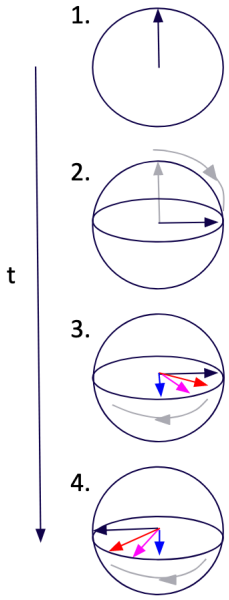

FIG. 2: Time evolution of nuclear spins in an echo pulse sequence. Step 1. Spins are polarized in the z-direction. Step 2. Coherent rotation into the xy plane. Step 3. Dephasing during spin precession in xy plane, shown in rotating frame of reference. Step 4. The phase of each of the spins is inverted and they begin to refocus.

By measuring the amplitude of this echo, one may extract valuable information about a sample's magnetic and electronic properties. Often, the main goal of Hahn echo experiments is to determine the decay of a nuclear magnetization. Longitudinal (T_1) and transverse (T_2) relaxation times are important characteristics of a material. T_1 is the process through which the nuclear magnetization recovers to its equilibrium state parallel to the external magnetic field after a RF pulse. T_2 describes the decay of the transverse magnetization due to spin-spin interactions in the system. T_2^* is the combined effect of T_2 and additional inhomogeneities, the latter of which can be refocused with a t_{180} pulse.

Employing a Discrete Fourier transform to the echo measurements unveils the precise frequencies of the nuclear spins that contribute to the resultant echo. While a simplified scenario envisions a spectrum that prominently spikes at the Larmor frequency with minimal width, reality introduces a spectrum with a width governed by dipole broadening and other decoherence effects. By utilizing quadrature detection of the real and imaginary parts of the echo signal, we can gain phase

information in the FFT. This concept is pivital in our study.

Experiment

We aim to perform NMR using traditional Hahn echo pulse sequences, but while also applying a pulsed, tetragonal symmetry-breaking strain field. A similar experiment has already been done using static strain fields, so we inherit multiple characteristics from that set-up. To apply strain, we employ a RazorbillTM CS100 piezoelectric device seen in Fig 3. A voltage difference is applied across the piezoelectric stacks, resulting in a contraction or stretching of the sample.

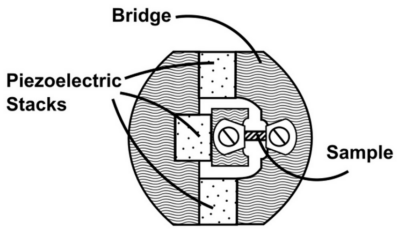

FIG. 3: Geometry of the piezoelectric device.

We calculate the actual displacement of the sample by measuring the capacitance of the system and calibrate what strain is applied for a given voltage. The piezo stacks have four connections total and we utilize the connections to apply a steady DC voltage in addition to our pulsed voltage sequence. By using proportional integral derivative (PID) control, we can maintain the same static displacement using just two of the piezo connections. The pulsed sequence is applied on top of this static voltage using the final two connections to ensure that there is no drifting from the original displacement as the experiment evolves.

The piezo device and sample is subsequently positioned onto a probe and gently lowered into our Oxford magnet. Employing a superconducting coil that carries 120 A, the magnet generates a magnetic field of around 11.7 T. At the site of the sample, this field is extremely uniform and is thus suitable for high-precision NMR measurements. To maintain the superconductivity of the coils, the magnet is comprised of multiple nesting layers filled with cryogens, with liquid Helium surrounding the coils. The temperature at the sample location is independently controlled.

The ^{75}As quadrupolar moment couples with the EFG, making it a sensitive probe to the Fe d-orbital occupations. Applying strain to $BaFe_2As_2$ causes the lattice to shift, physically changing the locations of the ions and thus changing the EFG at ^{75}As sites. This change is reflected in the quadrupolar splitting. The change in η due to strain is known as the nematic susceptibility of a nucleus. In the static strain experiment, the susceptibilities were plotted as a function of temperature and the values diverged near the structural transition (Fig 4). These data points matched other methods of measuring nematic susceptibility and are the result we aim to recreate with the new technique.

Static strain directly changes the splitting and therefore the resonance frequency of the satellite transitions. We measure this splitting as a proxy for the EFG. In contrast, pulsed strain will not shift the resonance frequency of a satellite transition as we vary the magnitude. Instead it will change the phase of the x and y signal frequencies that arise from the precession of the nuclear spins.

Qutip Simulations

Using simulations, we aim to show that this phase difference is expected and measurable. Qutip, a quantum toolbox in python, is a common library that can simulate the time evolution of quantum systems [5]. We utilize the master equation solver, which solves the time dependent Schrodinger equation over the duration of a given time list in specified step sizes. It's easiest to separate our Hamiltonian into time-dependent and time-independent parts, where the time-independent term is given as the Zeeman Hamiltonian.

$$H_i = -\gamma\hbar H_0 \hat{I}_z = \omega_0 \hat{I}_z \tag{6}$$

Where γ is the gyromagnetic ratio (usually in units of $\frac{MHz}{T}$), $\hbar$ is the reduced Planck's constant, H_0 is the external magnetic field, and $\hat{I}_z$ is the spin z operator. The quadrupolar term, which couples to our strain pulse, is slightly more complicated. It introduces the asymmetry parameter η used to model strain in our simulation. For the sake of the simulation, the rf and strain pulses are not applied at the same time. The quadrupolar Hamiltonian contributions are:

$$H_{dx} = V_{zz}\frac{\eta - 1}{2}(3\hat{I_x}^2 - \hat{I}^2) \tag{7}$$

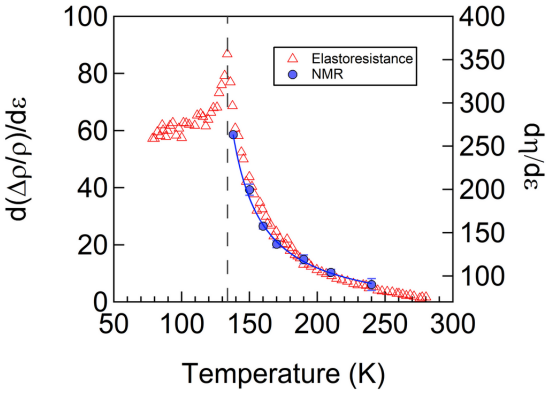

FIG. 4: Used with permission from [2]. The nematic susceptibility measured by static strain vs temperature. Results match the measurements made by elastoresistance (reproduced from [3]). The solid line is a fit to the NMR data. The vertical dashed line indicates the temperature of the nematic transition given by the fit [2].

$$H_{dy} = V_{zz}(3\hat{I_y}^2 - \hat{I}^2) \tag{8}$$

$$H_{dz} = -V_{zz}\frac{(\eta+1)}{2}(3\hat{I_z}^2 - \hat{I}^2) \tag{9}$$

where $\hat{I}_y$ is the spin y operator, $\hat{I}_x$ is the spin x operator, and $\hat{I}^2 = I(I+1)$ multiplied by the identity matrix. The Hamiltonian is split into parts based on spin operator for visualization purposes. Finally, we must model the RF pulse as a change to this time-dependent component. To do this we simply designed a Hahn echo sequence of pulses that would act on $\hat{I}_x$, as the RF pulses are applied in the x direction for our real experiment.

It is not immediately obvious how long the RF pulse needs to be applied in order for the spins to rotate by 90 and then 180 degrees. For these reasons we ran a series of simulations that acted as a nutation experiment for this t_{90} time. Qutip has the ability to track the expectation values of the spins in each direction. This is done with η set equal to zero. In order for us to claim that the spins have dropped into the xy plane, we must see the spin z expectation value reach the average of the two superimposed spin states.

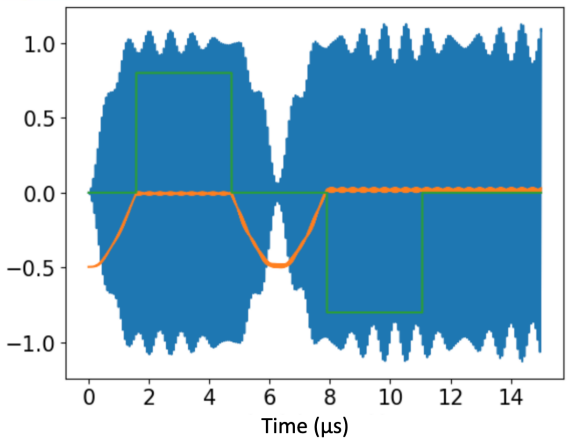

FIG. 5: Spin z (orange) and spin x (blue) expectation values as a function of time with strain pulse included (green). The x axis is time in units of microseconds, set by the units of the given gyromagnetic ratio.

For example, if we were probing the central transition of an As nucleus then the spins go from being polarized in either the spin $\pm\frac{1}{2}$ state (depending on the sign of γ) to a nearly equal superposition of both. This can be observed as the moment when the expectation value for spin z becomes zero.

The t_{180} pulse is applied for twice as long as the first, but will be of slightly different phase. Fig 5 shows the inverting of nuclear spins due to the t_{180} pulse in addition to the initial t_{90} pulse that forces the spins to the xy plane. We combine the magnetization in the x and y directions to create a complex signal before taking the Discrete Fourier transform. The result can be split into a real and imaginary spectrum representing the precession frequency of spin x and spin y respectively. To measure the effect of strain pulses, we ran a series of simulations where $\eta \in (-0.002, -0.001, 0, 0.001, 0.002, 0.003)$ and a subset of the spectra are shown in Fig 6.

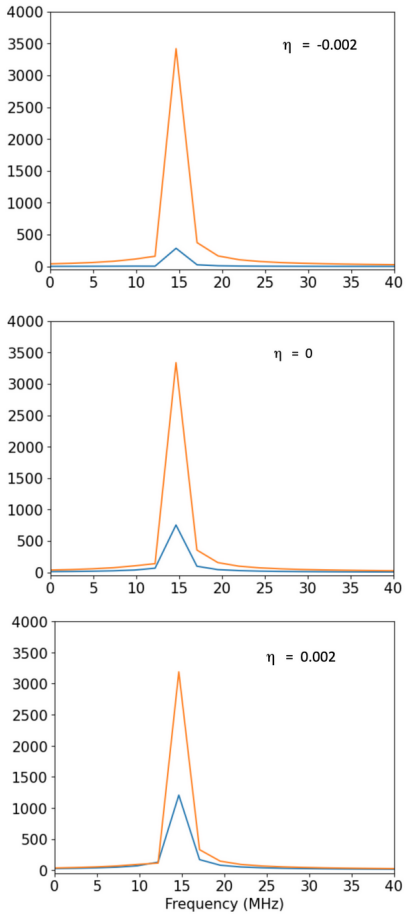

FIG. 6: Real (blue) and Imaginary (orange) spectra for $\eta = -0.002$, $\eta = 0$, and $\eta = 0.002$. The horizontal axis measures frequency in MHz while the vertical axis measures some unit of intensity.

Indeed we see a phase in the real and imaginary spectra despite not applying enough strain to produce a measurable shift in the resonance frequency. The phase shift, θ, is related to the frequency shift, Δf, by $\theta = 2(\Delta f)\tau$

Results

Fig 7 shows the spectrum of the imaginary signal for eleven different piezo voltages at room temperature. The phase falls behind as the positive pulses become higher voltage, but jumps ahead as the negative pulses become more negative.

We have shaped the pulses to be more square since this initial measurement, striking a balance between the length of time strain is applied (which makes our analysis more accurate) and the decay constant T2, and hence this value was used in the minimum strain calculations. The change in phase has a linear relationship with the applied strain pulse, just as the frequency change responded linearly to static strain. When we run this experiment at multiple PID controlled temperatures, we notice that the slope of this response grows as we lower the temperature. Our results are plotted next to the static strain data in Fig 8.

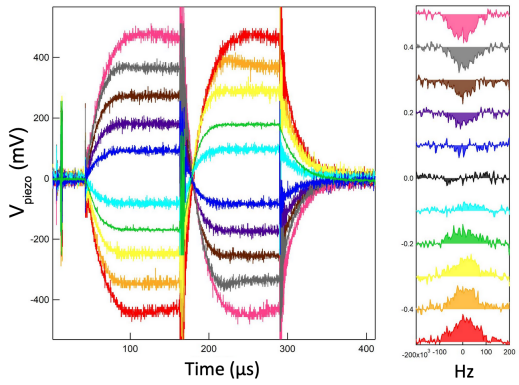

FIG. 7: Left: Voltage across piezo device as a function of time. Right: Phase of the imaginary spectra.

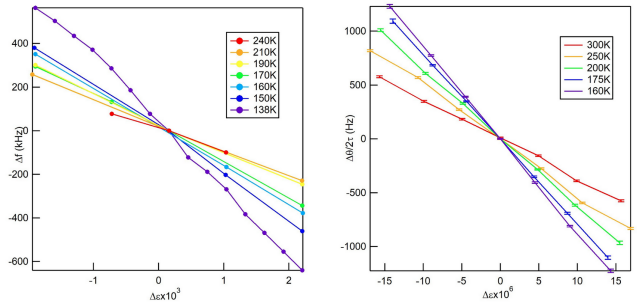

FIG. 8: Left: Change in satellite resonance frequency as a function of static strain. The vertical axis is given in kHz and the horizontal axis is strain multiplied by 10^3. Right: Calculated frequency change as a function of pulsed strain. The vertical axis is given in Hz and the horizontal axis is the magnitude of pulsed strain multiplied by 10^6

Our experiment was run over a similar temperature range and we successfully observe the same behavior as the static strain method with increased sensitivity. Instead of requiring static strain on the order of 10^{-3}, the pulsed technique measures the same slopes using only 10^{-6} strain. While we did cover a larger range of applied strain, taking more measurements within a smaller range would have yielded the same slope, so we retain the three orders of magnitude in increased sensitivity. We expect the nematic susceptibility to behave similarly to the magnetic susceptibility of an antiferromagnet above the Curie temperature, so we compare the techniques is by fitting nematic susceptibilities as a function of temperature to a Curie-Weiss form (Fig 9). It is clear that the two fits are off by a constant factor. We have not yet measured the total sample length accurately, so all calculations were done assuming a length of 1mm. Should it turn out that the crystal is closer to 2mm, the Curie-Weiss fits fall almost perfectly on top of one another.

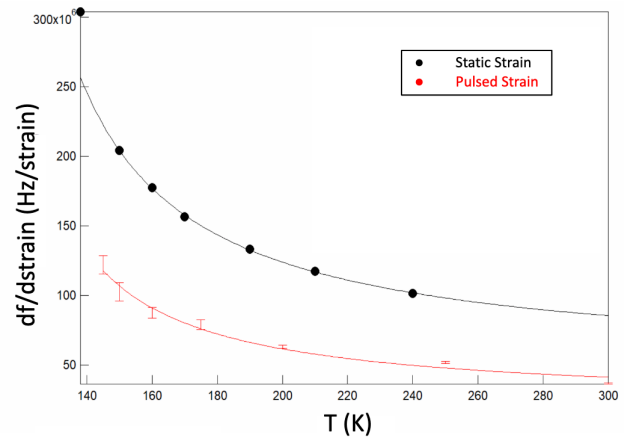

FIG. 9: Static strain fit recreated with permission from [2]. Pulsed and Static strain slopes fit to Curie-Weiss function.

Conclusion

In summary, our investigation has included a comprehensive exploration of the EFG under the influence of uniform uniaxial strain, employing a novel approach utilizing pulsed strain dynamics. This departure from the static strain method may yeild remarkable improvements in sensitivity, enhancing our ability to measure small changes in the EFG at nuclear sites. Most notably, our pulsed strain technique requires three orders of magnitude less strain to reproduce static strain results.

Our findings, in line with those presented in the previous study on static strain in $BaFe_2As_2$, unveil a linear response to strain that is tied to temperature. Consistent with other methods of measuring nematic susceptibility, strain measurements observe the broken C_4 symmetry and the resulting impact on Fe 3d and ^{75}As 4p orbital occupations. Unlike traditional methods such as elasto-resistance and Raman scattering, our pulsed strain NMR is uniquely poised to explore nematic susceptibility even in the superconducting state, providing an opportunity to gain insights into the interplay between nematic degrees of freedom and the underlying superconducting and magnetic ordering mechanism.

[1] Kissikov, T. Curro, N.J. “Uniaxial strain control of spin-polarization in multicomponent nematic order of BaFe2As2” *Nature Communications* **9**, 1058 (2018).

[2] Kissikov, T. Sarkar, R. Lawson, M. et al “Local nematic susceptibility in stressed BaFe2As2 from NMR electric field gradient measurements” *Physical Review B* **96**, (2017).

[3] Jiun-Haw Chu, Hsueh-Hui Kuo, James G. Analytis. “ Divergent nematic susceptibility in an iron arsenide superconductor” *Science 337*, 710 (2012)

[4] Curro, N.J. “ Nuclear Magnetic Resonance as a Probe of Strongly Correlated Electron Systems”

[5] J. R. Johansson, P. D. Nation, and F. Nori: ”QuTiP 2: A Python framework for the dynamics of open quantum systems.”, Comp. Phys. Comm. 184, 1234 (2013)